ACS Sustainable Chemistry & Engineering

pubs.acs.org/journal/ascecg

Research Article

Single-Pass Electrooxidation of Glycerol on Bismuth-Modified Platinum Electrodes as an Anodic Process Coupled to the Continuous CO_2 Electroreduction toward Formate

Published as part of ACS Sustainable Chemistry & Engineering virtual special issue "Sustainable Energy and CO_2 Conversion - Angel Irabien Festschrift".

Ailen Peña-Rodríguez, Kevin Fernández-Caso, Guillermo Díaz-Sainz, Manuel Álvarez-Guerra, Vicente Montiel, and Jose Solla-Gullón*

Cite This: ACS Sustainable Chem. Eng. 2024, 12, 3671−3679

Read Online

ACCESS | Metrics & More | Article Recommendations | Supporting Information

ABSTRACT: CO_2 electroreduction has emerged as a promising strategy for reducing emissions while simultaneously generating valuable products, particularly formic acid/formate. To further enhance the sustainability of this process, the traditional oxygen evolution reaction at the anode can be replaced by a more interesting reaction like glycerol oxidation to high value-added products, in a covalorization approach. In this study, the effect of the presence of a bismuth (Bi) atom supplier (Bi_2O_3 particles) in the anolyte solution during the glycerol electrooxidation process on platinum (Pt) electrodes coupled with the electroreduction of CO_2 to formate is investigated for the first time, operating in a continuous mode with a single pass through the reactor. The results reveal that in the cathode, significant $HCOO^-$ production, with Faradaic efficiencies reaching 93%, and modest energy consumption of 208 kW h·kmol^{-1} were obtained in the continuous CO_2 electroreduction to formate using Bi gas diffusion electrodes. On the other hand, in the anode, the presence of Bi_2O_3 particles leads to a significant alteration in the distribution of high-value-added oxidation products obtained. For instance, the anode demonstrates remarkable dihydroxyacetone (DHA) production of 283 μmol·m^{-2}·s^{-1}, surpassing the results obtained with the nonmodified Pt electrodes. The performance of this system offers a promising pathway for the simultaneous coproduction of high-value-added products from both CO_2 and glycerol.

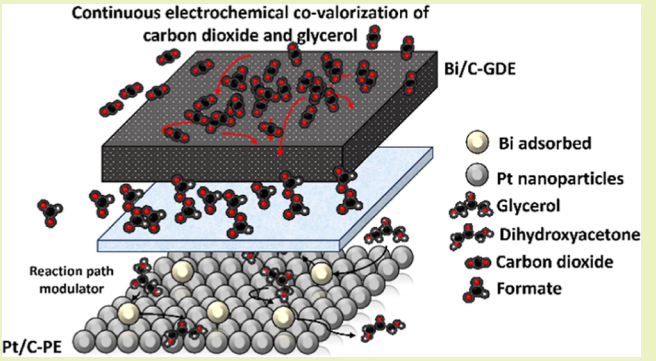

KEYWORDS: *single-pass glycerol oxidation reaction, bismuth-modified platinum electrodes, high-value-added product, continuous CO_2 electroreduction, formate, Bi gas diffusion electrodes*

1. INTRODUCTION

The electrochemical reduction of CO_2 (CO_2RR) is the subject of countless contributions. This is because this process is a very promising and attractive technology to convert CO_2 into valuable chemicals and fuels using renewable electricity. In this sense, in 2022, some of the most relevant researchers on the topic reported a roadmap in which they analyzed and discussed some relevant and recent advances in different aspects, including progress not only on the fundamental understanding of the reaction and the development and properties of new electrocatalysts but also on the issues and challenges related to the engineering and scaling-up of the process that can remarkably contribute toward the future commercialization of the CO_2RR technology.[1] During this last year, the increasing interest in this process has continued and, as proof of this, numerous and relevant reviews and articles dealing with the CO_2RR have been published.[2−23] In addition, due to their interesting and practical applications, the electrochemical reduction of CO_2 to formic acid/formate has been extensively studied.[5,24−30] It is also widely accepted that for future practical and industrial implementation of the CO_2RR technology, the use of electrochemical reactors working in continuous operation mode is more convenient.[5,31,32] Besides, the employment of continuous flow conditions for electrochemical reactions has shown to provide relevant benefits over

Received: October 31, 2023
Revised: January 30, 2024
Accepted: February 12, 2024
Published: February 21, 2024

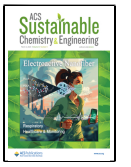

batch conditions, including not only better Faradaic efficiencies (FEs), higher selectivities, lower electrolyte loadings, and reduced energy consumption (EC) but also an improved control of the process and less difficulties for a subsequent scale-up.[33] Particularly for CO_2 electroreduction, working in continuous operation mode also significantly contributes to minimize the limitations attributed to mass transport, which allows reaching higher CO_2 conversion rates.[31] In consequence, in recent years, relevant contributions have been reported dealing with the continuous CO_2 electroreduction to high-added-value products.[5,34−36] For instance, Fernández-Caso et al.[5] reviewed the electroreduction of CO_2 to $HCOO^-$ or HCOOH operating in continuous mode and quantitatively compared the performance of the different approaches in terms of the relevant figures of merit used (current density, $HCOOH/HCOO^-$ concentration, FE, production rate, and EC).

On the other hand, the oxygen evolution reaction (OER) has been typically the anodic half-cell reaction used in the CO_2RR. However, the sluggish kinetics of the OER and the low industrial value of the O_2 produced at the anode significantly reduce the competitiveness and economic feasibility of this process. In this way, coupling more valuable anodic reactions with CO_2 electroreduction has been the subject of recent and valuable contributions[37−52] and has emerged as a promising approach to lower the overall cell voltage, and consequently the energy efficiency of the system, and also to simultaneously produce high-added-value products both at the cathode and anode. Among the different anodic processes used as paired reactions with CO_2RR, the electrooxidation of glycerol (GOR, glycerol oxidation reaction) to high-added-value products is one of the most interesting alternatives.[38,41,43,46,51−53] Glycerol is the major waste product from biodiesel production and can be electrochemically oxidized into a variety of valuable chemicals.[54−57] In this sense, Verma et al.[38] demonstrated that coupling CO_2RR with the electrooxidation of glycerol reduced the power consumption of the system by 53% compared to use of the OER as anodic process. More recently, Junqueira et al.[43] reported the simultaneous production of formate both at the anode and cathode from the paired CO_2RR and glycerol electrooxidation at high currents (200 mA cm^2) with FEs of about 96 and 45% at the anode and cathode, respectively. Interestingly, Rumayor et al.[58] showed that the coproduction of $HCOO^-$ and dihydroxyacetone (DHA) from the CO_2RR and glycerol electrooxidation, respectively, can be economically feasible for DHA concentrations higher than 1.5 wt % in the anode.

Regarding the electrooxidation of glycerol, noble metal electrocatalysts are the most explored ones.[57,59−62] In particular, Pt and Pt-based electrocatalysts have been widely used in the literature due to their high activity at different pH conditions. However, its high bond-breaking ability is inconvenient for the obtention of C2 and C3 oxidation products and is also easily poisoned by the CO and other intermediates generated during the glycerol electrooxidation. Among other strategies to overcome these limitations, the use of certain adatoms to decorate the surface of the Pt electrodes and consequently modifying their electrocatalytic properties have been reported to be an interesting approach.[63−68] For instance, Bi-modified Pt electrodes, including polyoriented and single crystal electrodes, and Pt nanoparticles, displayed interesting properties toward glycerol electrooxidation in an alkaline solution both in fundamental electrochemical experiments[66,67] and in 3D-printed microfluidic fuel cell devices.[69] In this context, in this work, we explore the single-pass and continuous electrooxidation of glycerol on bismuth-modified platinum electrodes as an anodic process coupled to the continuous CO_2 electroreduction toward formate. As previously discussed by De Souza et al.,[66] it is more convenient to directly add a Bi atom supplier (in this case, Bi_2O_3 particles) into the anodic solution to avoid the clear deactivation of the Bi decoration that it is observed when the Pt surface is modified by irreversible adsorption of Bi. In addition, the results obtained will be analyzed and compared with some of our previous findings in which the OER and the glycerol electrooxidation (in absence of Bi) were employed as anodic reactions, while the continuous CO_2 electroreduction toward formate remained unmodified.[35,36]

2. EXPERIMENTAL SECTION

2.1. Preparation and Characterization of the Electrodes. Details regarding the synthesis and characterization of the carbon-supported Bi nanoparticles (Bi/C NPs) used as cathode electrocatalysts, as well as the subsequent fabrication and characterization of the gas diffusion electrodes incorporating these Bi nanoparticles (Bi/C-GDE), can be found in some of our previous publications.[70,71] In brief, Bi/C-GDE is composed of a carbonaceous support (Teflonated Toray carbon paper TGP-H-60), a microporous layer (MPL), and a catalytic layer (CL). The MPL ink was prepared by combining Vulcan XC-72R and poly(tetrafluoroethylene) (PTFE preparation, 60 wt % dispersion on H_2O, Sigma-Aldrich) in a mass ratio of 40/60, and then diluted in isopropanol to achieve a final slurry of 3 wt %. The ink was sonicated for 30 min before it was sprayed with an airbrusher over the carbonaceous support. When the MPL reached a Vulcan XC-72R loading of 2 mg·cm^{-2}, both layers were sintered at 350 °C for 30 min. Subsequently, the CL was sprayed over the MPL using the same technique. The catalytic ink consisted of Bi/C NPs in Nafion (Nafion D-521 dispersion, 5 w/w % in water and 1-propanol, 0.92 mequiv·g^{-1} exchange capacity) with a mass ratio of 70/30, which was then diluted in isopropanol and sonicated in the same conditions as described previously for the MPL. The Bi/C NPs' loading was 0.75 mg·cm^{-2}, as in previous studies for the purpose of comparison.

The Pt particulate electrodes (Pt/C-PE) used as anode were prepared by direct deposition of the carbon-supported Pt nanoparticles (Pt/C) (20 wt %, particle size ≤5 nm, Sigma-Aldrich) onto a carbonaceous support (Teflonated Toray carbon paper TGP-H-60) using a similar methodology to that employed for the catalytic layer of the Bi/C-GDEs. The Pt loading deposited over the carbonaceous support was 1.00 mg·cm^{-2}. The physicochemical characterization of the Bi/C-GDE and Pt/C-PE was reported in some of our previous contributions.[41,71]

2.2. Experimental Setup for Flow Cell Tests. The Bi/C-GDE and Pt/C-PE were used as cathode and anode, respectively, in a continuous filter press electrochemical reactor. Each electrode had a geometric surface area of 10 cm^2. The experimental setup consisted of a filter press reactor as the core component, along with peristaltic pumps (Watson Marlow 320, Watson Marlow Pumps Group), tanks, and a potentiostat−galvanostat (Arbin Instruments, MSTAT4). The cathodic compartment of the electrochemical reactor was fed with a solution composed of 0.5 M KCl (potassium chloride, pharma grade, PanReac AppliChem) +0.45 M $KHCO_3$ (potassium hydrogen carbonate, pharma grade, PanReac AppliChem). Moreover, pure CO_2 was continuously supplied to the cathodic compartment at a flow rate of 200 mL·min^{-1}, similar as previous studies conducted by the group.[41,70−74]

On the other hand, the anolyte consisted of an aqueous solution of 1.0 M KOH (potassium hydroxide, 85% purity, pharma grade, PanReac AppliChem) +1.0 M GLY (glycerol, 99% purity, ReagentPlus, Sigma-Aldrich). About 150 mg of Bi_2O_3 particles (Bi_2O_3 powder, 99.999% trace metals basic) per liter (L) of anolyte was added into the anolyte feed tank, and the mixture was

https://doi.org/10.1021/acssuschemeng.3c07131
ACS Sustainable Chem. Eng. 2024, 12, 3671−3679

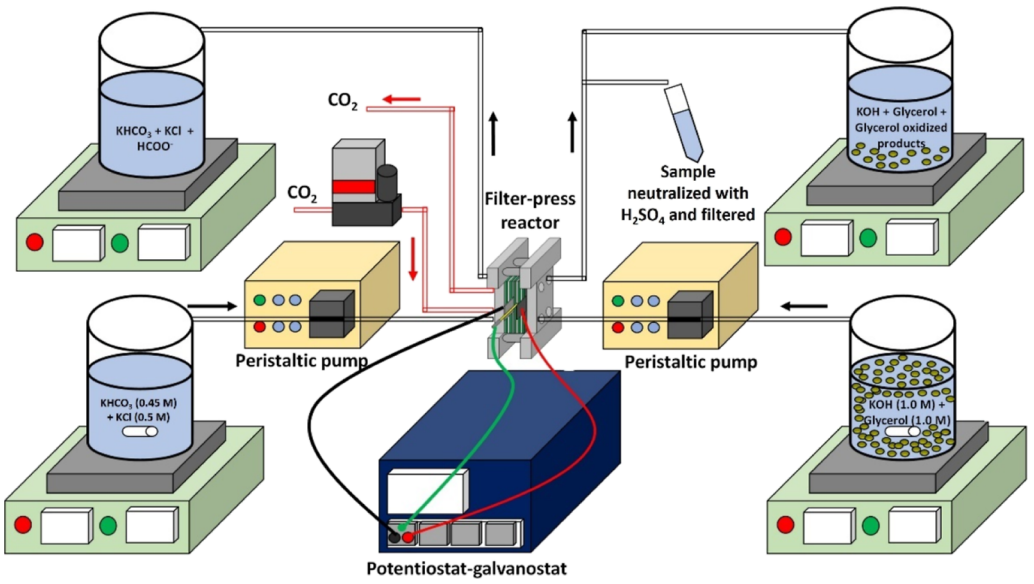

Figure 1. Experimental setup scheme employed for coupling the single-pass GOR to the continuous CO_2RR process to give $HCOO^-$.

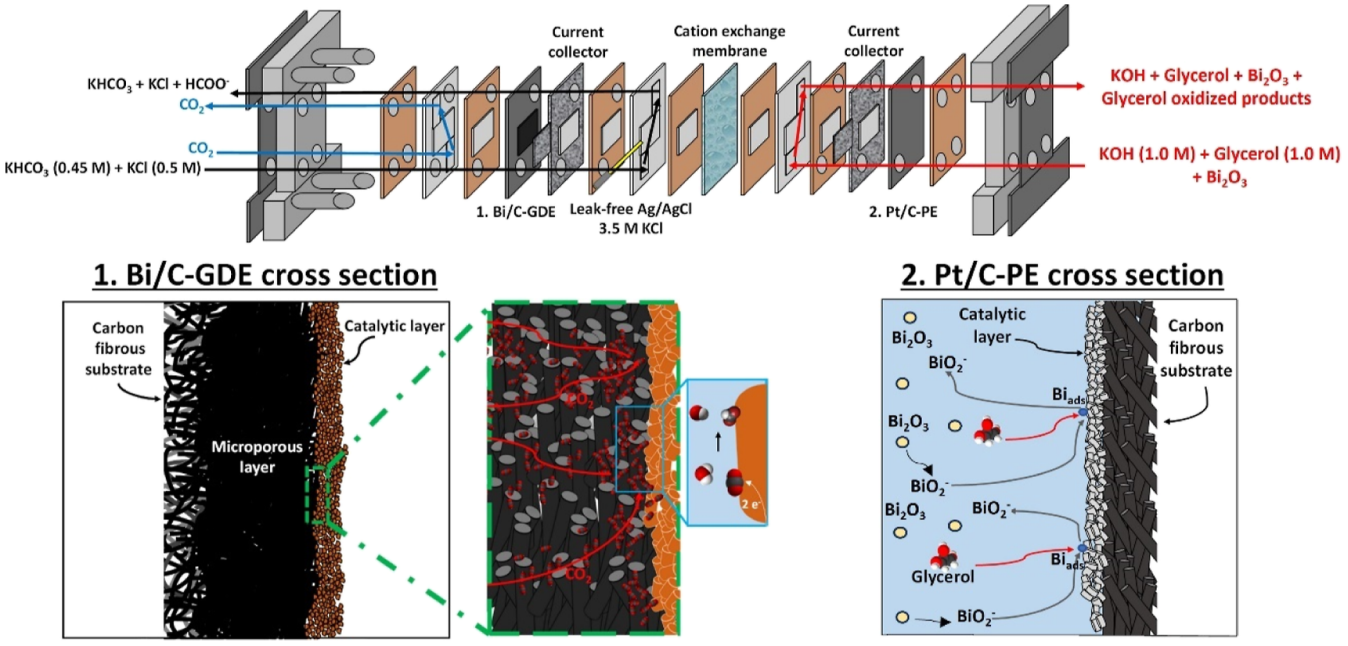

Figure 2. Schematic illustration of the filter press reactor with stacked components, indicating that the continuous CO_2 reaction to $HCOO^-$ takes place on the Bi/C-GDE surface (1) and the single-pass GOR on the catalytic layer of Pt/C-PE (2) in the presence of Bi_2O_3 particles as the Bi atom supplier.

magnetically stirred for 10−15 min before being directly pumped into the electrochemical reactor. These Bi_2O_3 particles in the solution act as a Bi atom supplier. About 2 L of anolyte was prepared per experiment. Figure 1 schematically represents the experimental setup employed in the flow cell experiments.

Figure 2 illustrates the internal structure of the filter press reactor configuration with stacked components (Micro Flow Cell, Electro-Cell, A/s). The cathodic and anodic compartments of the CO_2 electrolyzer are separated by a Nafion 117 cationic exchange membrane (Alfa Aesar). A leak-free Ag/AgCl 3.5 M KCl reference electrode was placed close to the working electrode in the cathodic compartment. All the experiments were performed in duplicate with a duration of 60 min, in continuous mode with a single pass of reactants through the electrochemical reactor in both the cathodic and the anodic compartments. Moreover, all the tests were carried out at ambient conditions of pressure and temperature. At every 15 min, the samples of the catholyte and anolyte were collected to measure the concentration of $HCOO^-$ and glycerol, respectively. Samples of the anolyte were neutralized using a 1.0 M H_2SO_4 solution (sulfuric acid, 98% purity, pharma grade, PanReac AppliChem) to immediately reduce the pH of the sample to about 2 and stop the Cannizzaro reaction between aldehydes and alcohols. This particularly facilitates the determination of the dihydroxyacetone (DHA) and glyceraldehyde (GLAD) concentrations in alkaline media. The sample was also filtered (nylon syringe filters, 0.22 μm) before being analyzed. The different analytical techniques employed for the quantification of the concentration of $HCOO^-$, glycerol, and the different oxidized products from GOR are summarized in the Supporting Information. The figures of merit calculated through the eqs S1−S10 were used for the performance assessment of the coupled electrochemical device implemented in this work.

https://doi.org/10.1021/acssuschemeng.3c07131
ACS Sustainable Chem. Eng. 2024, 12, 3671−3679

3. RESULTS AND DISCUSSION

3.1. Effects on the CO_2 Electroreduction to Formate.

In this section, we evaluate the effects of the presence of Bi_2O_3 particles in the anolyte during GOR on the performance of the continuous CO_2RR process to $HCOO^-$ in the cathode. To properly assess the effects of the presence of the Bi_2O_3 particles in the anolyte, the results obtained here have been compared with those obtained under the same experimental and operating conditions but in the absence of Bi_2O_3 particles in the anolyte and reported in some of our previous investigations.[41] Also, previous results obtained in comparable experimental and operating conditions but using the OER at commercial dimensionally stable anodes (DSA/O_2) (Ir-MMO (mixed metal oxide) on platinum) as anodic process have been included in this comparative analysis.[70] This comparative analysis is displayed in Figure 3 in which the performance of

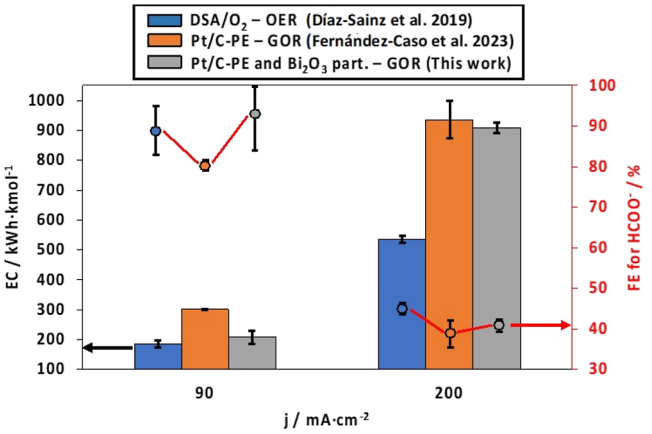

Figure 3. ECs per kmol of $HCOO^-$ [EC] and FEs for $HCOO^-$ [FE for $HCOO^-$] as a function of the current density supplied [j] obtained for the different works with the same experimental setup but different anode systems; Díaz-Sainz et al. 2019 (ref 70) with a commercial DSA/O_2 for the OER (in blue); Fernández-Caso et al. 2023 (ref 41) with a Pt/C-PE for the GOR (in orange); and Bi-modified Pt/C-PE for the GOR (this work, in gray).

the CO_2RR to $HCOO^-$ in terms of the EC per kmol of $HCOO^-$ [EC] and FE of $HCOO^-$ [FE for $HCOO^-$] attained in the cathode are compared. In addition, detailed results of the figures of merit, including the concentration ([$HCOO^-$]) and production rate (r$HCOO^-$) for this product, are summarized in Table S1.

The results shown in Table S1 indicate that, in the presence of Bi_2O_3 particles and working with a catholyte flow per geometric surface area of 0.15 mL·min^{-1}·cm^{-2} and a current density of −90 mA·cm^{-2}, high concentrations and production rates for $HCOO^-$ of about 7.9 g·L^{-1} and 4.37 mmol·m^{-2}·s^{-1}, respectively, were obtained in the cathode. These values are clearly better than those obtained in the absence of Bi_2O_3 particles (6.8 g·L^{-1} and 3.76 mmol·m^{-2}·s^{-1}, respectively) and also better than those using the OER as an anodic reaction (7.5 g·L^{-1} and 4.18 mmol·m^{-2}·s^{-1}). These results represent an increase of approximately 16% in comparison with those obtained in the absence of Bi_2O_3 particles, and about 4.5% in comparison with those obtained using the OER on a DSA/O_2 electrode. It is also worth noting that, in the presence of Bi_2O_3 particles, FEs toward $HCOO^-$ of up to 93% were also obtained. These FEs are higher than the FE values of 80 and 89% obtained in the absence of Bi_2O_3 particles and using the OER, respectively. It is also interesting to mention that, working at −90 mA·cm^{-2}, the high $HCOO^-$ production obtained at the cathode, together with a relatively low cell voltage of −3.62 V, allows achieving ECs of only 208 kW h·kmol^{-1}. This value represents a remarkable drop of about 30% compared to the EC obtained when Bi_2O_3 particles were not added to the anolyte (Figure 3).[41] This EC is similar to the value of 186 kW h·kmol^{-1} obtained when the OER on a DSA/O_2 electrode was used as a coupled anodic reaction.

As also shown in Table S1, for experiments performed at lower catholyte flow per geometric surface area (0.07 mL·min^{-1}·cm^{-2}) and more commercially relevant[5,75] current densities of −200 mA·cm^{-2}, the $HCOO^-$ concentrations obtained in the presence and in the absence of Bi_2O_3 particles on the anolyte were very similar, 16.40 vs 15.60 g·L^{-1}, respectively. In terms of FE toward $HCOO^-$, a value of 41% was obtained, which is also similar to that obtained in the absence of Bi_2O_3 particles (39%) and that obtained when the OER is used as the anodic reaction (45%), Figure 3. Under these high current density conditions, similar cell voltages were found in the absence (−6.94 V)[41] and in the presence (−6.91 V) of Bi_2O_3 particles in the anolyte (Table S1 of the Supporting Information). Consequently, similar ECs of 936 and 909 kW h·kmol^{-1} were obtained. However, as shown in Figure 3 and in Table S1 of the Supporting Information, these ECs are much higher than that obtained using the OER as an anodic reaction, which is only about 535 kW h·kmol^{-1} (−4.67 V).

These results indicate that, at a current density of −90 mA·cm^{-2}, when Bi_2O_3 is added in the anolyte, the figures of merit reported for the CO_2 electroreduction showed an interesting improvement in comparison with previous findings when the GOR in the absence of Bi_2O_3 or the OER was used as coupled anodic reactions. Nevertheless, this improvement is not observed at the higher current densities of 200 mA·cm^{-2}. At these high current densities and despite the results in terms of $HCOO^-$ production, FE, and ECs being similar in the absence and presence of Bi_2O_3 for the GOR, these are clearly worse than those observed when the OER is the coupled anodic reaction.

3.2. Effect of Addition of Bi_2O_3 Particles in the Anolyte in the Continuous Electrooxidation of Glycerol.

This section will be mainly focused on the effect of the incorporation of Bi_2O_3 particles in the anolyte on the distribution of products obtained in the continuous electrooxidation of glycerol in alkaline solution coupled to the electroreduction of CO_2 to formate. As in the previous section, the results obtained will be compared with those previously reported in comparable experimental and operating conditions but in the absence of the Bi_2O_3 particles in the anolyte.[41] All experiments were performed at an anolyte flow rate per geometric anode surface area (Q_a/A) of 1.71 mL·min^{-1}·cm^{-2}. As reported in this previous contribution,[41] the relatively high anolyte flow rate values of up to 1.71 mL·min^{-1}·cm^{-2} allowed us to maximize the formation of DHA in the output anolyte stream, since this compound can suffer a degradation reaction in highly concentrated alkaline environments, and therefore, it is important to reduce the DHA residence time in the alkaline anolyte before its neutralization with the acidic solution.[41,66]

Before describing the main results obtained during the flow electrochemical experiments and to better understand the effect of the presence of Bi_2O_3 on the electrooxidation of glycerol in an alkaline solution on Pt electrodes, some

https://doi.org/10.1021/acssuschemeng.3c07131
ACS Sustainable Chem. Eng. 2024, 12, 3671−3679

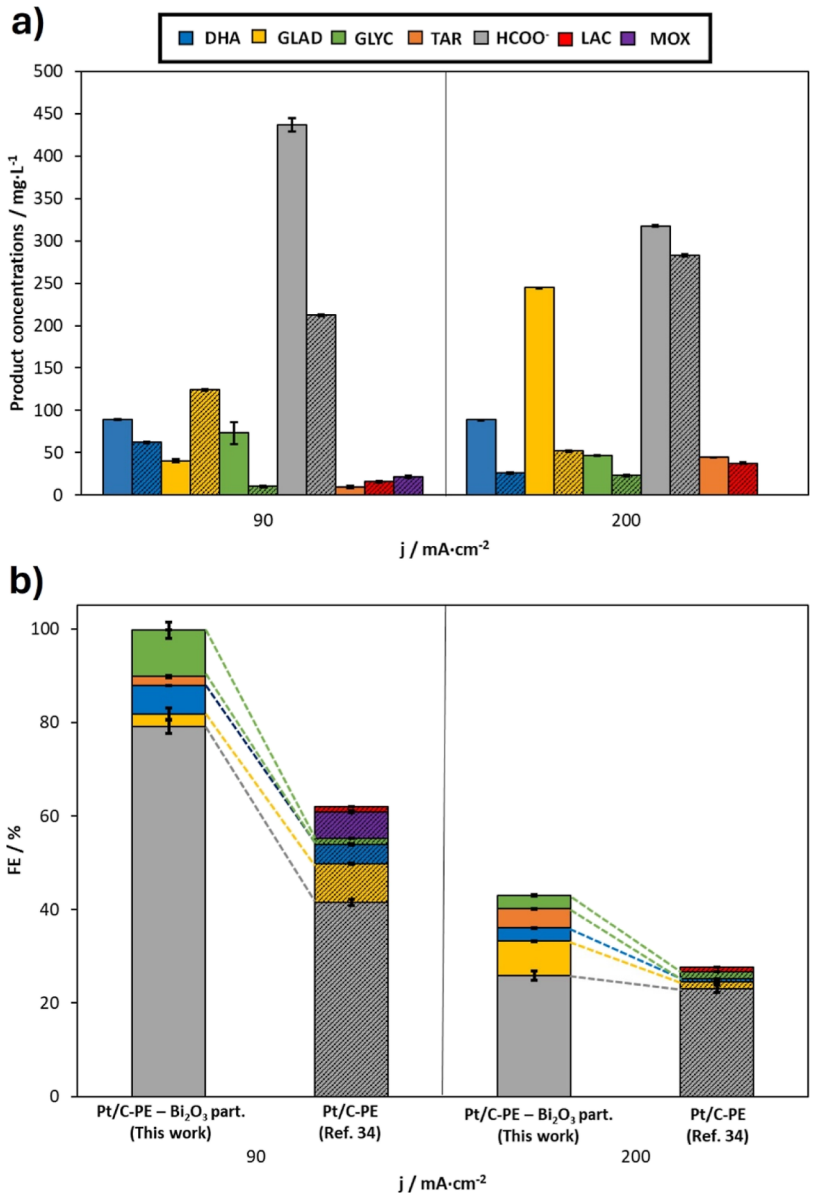

Figure 4. (a) Concentrations and (b) FEs of the different oxidized products from GOR in output anolyte stream when the Pt/C-PE was employed in the presence of Bi_2O_3 particles (this work as nonstriped bars) and previous approach with the Pt/C-PE (ref 34 as stripped bars) as a function of the current density (j) supplied to the filter-press reactor.

preliminary voltammetric experiments were performed. Figure S1 shows the results obtained. Figure S1a displays the voltammetric response of a portion (geometric area of about 1 cm^2) of the Pt/C-PE electrode in 0.5 M H_2SO_4 solution. As expected, the voltammetric features observed are characteristic of a clean and polyoriented Pt surface.[76,77] The electroactive surface area (ECSA) of the Pt/C-PE electrode was estimated from the charge involved in the so-called hydrogen region, assuming a value of 0.21 mC cm^{-2} for the total charge after the subtraction of the double-layer charging contribution.[76,77] For a portion of the electrode of about 0.25 cm^2 (geometric area), a value of about 27 cm^2 of the ECSA was obtained, that is, about 108 cm^2 (ECSA) per cm^2 (geometric area). Figure S1b shows the voltammetric responses for the electrooxidation of glycerol in the presence and in the absence of Bi_2O_3 as the Bi atom supplier. In these voltammetric experiments and similar to the flow cell experiments (see the Experimental Section), before the electrochemical experiments, a certain amount of Bi_2O_3 particles was added into the solution and magnetically stirred for 10 min before being used. Inductively coupled plasma optical emission spectrometry (ICP-OES) (PerkinElmer, Optima 4300 D) measurements indicated that the concentration of Bi dissolved in solution from the Bi_2O_3 particles is about 30 ppm during the experiments. It is also worth noting that, as previously reported by Vivier et al.,[78] the Bi_2O_3 particles are partially dissolved into ionic BiO_2^- species in the alkaline solution, which are subsequently adsorbed and converted into Bi adsorbed species. Figure S1b shows that the addition of Bi_2O_3 particles shifts the onset potential of the oxidation of glycerol by about 200 mV to lower potentials. Similar observations have been reported in previous contributions.[65−67,69,79] This is due to the irreversible adsorption of Bi adatoms at the surface of the Pt nanoparticles, which is well-known to enhance the electrocatalytic properties of Pt for many different processes including glycerol electrooxidation.[64−67,69]

https://doi.org/10.1021/acssuschemeng.3c07131
ACS Sustainable Chem. Eng. 2024, 12, 3671−3679

For the experiments performed in continuous operation of the filter press reactor at a current density of 90 mA·cm^{-2}, Figure 4a, the addition of Bi_2O_3 particles allowed increasing of the DHA concentration from 62 (in the absence of Bi_2O_3 particles) to 89 mg·L^{-1}, which represents an increase of up to 43%. This increase represents an interesting FE of about 6% (Table S2 of the Supporting Information). Working at these operating conditions of 90 mA·cm^{-2}, GLAD, as the other intermediate of the GOR, was obtained with low concentrations of only 40 mg·L^{-1} in the output anolyte stream compared with the value of 124 mg·L^{-1} obtained in the absence of Bi_2O_3 particles (Figure 4a). Both intermediates are in equilibrium (isomerization reaction),[80] and the presence of higher amount of DHA justifies the minor GLAD formation.[41,65,66] Thus, the FE for GLAD is 2.75%, almost 66% lower than that obtained in the absence of Bi_2O_3 particles in the anolyte (Table S3). It is worth noting that tartronate (TAR), a three-carbon GOR product, was detected under these operating conditions of 90 mA·cm^{-2}. This finding contrasts with our previous results without Bi_2O_3.[41] TAR formation comes from the subsequent oxidation of the glycerate (GLCA) anion, which in turn comes from GLAD oxidation. This chemical route justifies the low GLAD concentrations detected.[81−83] The low TAR concentrations of about 10 mg·L^{-1} (Figure 4a) and the eight electrons involved in the corresponding oxidation reaction give rise to FE toward this product of about 2% (Table S4). Another chemical route for further oxidation of the GLAD intermediate involves the production of glycolate (GLYC) from the GLCA anion. This two-carbon compound (GLYC) can be formed with concentrations and FE of 73 mg·L^{-1} and 9.9%, respectively (Table S5 of the Supporting Information). These results again contrast with those obtained in the absence of Bi_2O_3 particles and point out the improvement in the formation of the GLYC anion instead of the formation of the GLAD intermediate. In addition, another interesting compound formed through this chemical route involves the $HCOO^-$ production, which is found to be the main oxidized product quantified from the GOR with a concentration and FE of up to 437 mg·L^{-1} and 80%, respectively (Figure 4a,b). At current densities of 90 mA·cm^{-2}, the $HCOO^-$ production was increased in the presence of Bi_2O_3 particles by up to 106% (Table S6 of the Supporting Information). The analytical quantification of all these oxidized products from GOR as well as the calculation of their corresponding FEs, allowed us to estimate a carbon balance of 6.94% and an overall FE of 99.80%, working at 90 mA·cm^{-2}. These findings indicate that most of the carbon products have been successfully identified (Table S7).

Similar experiments were conducted at a more commercially relevant current density of 200 mA·cm^{-2}. Similar to the experiments performed at 90 mA·cm^{-2}, $HCOO^-$ was again found to be the main oxidized product from GOR, although lower amounts of other oxidized products such as DHA, GLAD, and GLYC were also detected (Figure 4a). At these high current densities, the addition of Bi_2O_3 particles into the anolyte solution did not lead to a significant drop of the anode potential (Table S1 of the Supporting Information), in comparison to that in the previous experiments at 90 mA·cm^{-2}, and a similar high cell voltage of up to −6.91 V was found, which is mainly attributed to the high anode potential (4.99 V vs Ag/AgCl). In terms of product distribution, at 200 mA·cm^{-2}, the DHA concentration obtained drastically increased from 26 to 88 mg·L^{-1} (Figure 4a) in the presence of Bi_2O_3 particles, thus leading to an FE of about 2.7% (Figure 4b). Although DHA can be formed in higher amounts at these current densities, the reoxidation of this compound into other more oxidized ones can also occur. Interestingly, as shown in Figure 4a,b and in Table S3, the results also indicate a remarkable increase in the formation of the GLAD in the presence of Bi_2O_3 particles. The GLAD concentration and FE increase from 52 to 245 mg·L^{-1} and from 1.5 to 7.5%, respectively. Regarding the production of TAR, a significant improvement is observed. The results obtained show that the TAR concentration and FE also increase from 9.6 to 44 mg·L^{-1} and from 2 to 4%, respectively, when the current density is increased from 90 to 200 mA·cm^{-2}. A similar enhancement is again detected for GLYC concentrations and its FE, which increase up to 46 mg·L^{-1} and 2.8%, respectively, in the presence of Bi_2O_3 particles in comparison with the 23 mg·L^{-1} and 1.4%, respectively, reported in the absence of Bi_2O_3 particles under similar experimental and operating conditions. Finally, the results obtained at 200 mA·cm^{-2} evidence that although $HCOO^-$ still is the main oxidized product, both the $HCOO^-$ concentration and FE significantly decrease in comparison with the results obtained at 90 mA·cm^{-2}. The results show a $HCOO^-$ concentration and FE of about 317 mg·L^{-1} and 25%, respectively. These values are rather similar to those observed at the same current density (200 mA·cm^{-2}) but in the absence of the Bi_2O_3 particle in which values of about 283 mg·L^{-1} and 23%, were obtained, respectively. However, as shown in Figure 4b and Table S6, the FE toward $HCOO^-$ decreases from 79 to 25% when the current density is increased from 90 to 200 mA·cm^{-2}. In this sense, it is also worth noting that, as shown in Table S7, the glycerol conversion decreased from 7.47 (at 90 mA·cm^{-2}) to 5.14% (at 200 mA·cm^{-2}). This finding suggests that the parasitic OER seems to be enhanced at a major degree instead of GOR (which is thermodynamically more favorable) at these more positive anode potentials of up to 4.99 V vs Ag/AgCl, which justifies obtaining higher glycerol concentrations at 200 mA·cm^{-2} than at 90 mA·cm^{-2} in the output anolyte stream, as illustrated in Figures S2 and S3 of the Supporting Information. Also, considering this finding, the carbon balance and overall FE estimated for the experiments at relevant current densities of 200 mA·cm^{-2} were 4.46 and 43.0%, respectively (Figure S4 and Table S7).

In this work, the effects of the presence of Bi_2O_3 (acting as Bi atoms supplier during the experiments) in the anolyte in the single-pass electrooxidation of glycerol on platinum electrodes coupled to the continuous CO_2 electroreduction toward formate have been shown. The results obtained indicate that the continuous CO_2 electroreduction toward formate displays a slight improvement in terms of EC, FE, and $HCOO^-$ concentration in comparison with the results obtained in the absence of Bi_2O_3. However, in comparison with the use of the OER as coupled anodic reaction, the GOR is still noncompetitive at high current densities of −200 mA·cm^{-2}, although interesting results were observed at −90 mA·cm^{-2}. Regarding the single-pass electrooxidation of glycerol on platinum electrodes in alkaline solution, the results clearly show that the presence of Bi_2O_3 significantly modifies the distribution of products obtained also including the detection of products (TAR), which are not observed in the absence of Bi_2O_3. Also, interesting findings were obtained at 90 mA·cm^{-2} in terms of accumulated FE (almost 100%) although this

https://doi.org/10.1021/acssuschemeng.3c07131
ACS Sustainable Chem. Eng. 2024, 12, 3671−3679

significantly decreases to about 43% at higher current densities (200 mA·cm^{-2}).

4. CONCLUDING REMARKS

The innovative continuous system developed in this work has led to a more relevant modification of the distribution of glycerol oxidation products compared to that in our previous work.[41] The presence of Bi_2O_3 (acting as a Bi atom supplier during the experiments) in the anolyte has resulted in the higher production of three carbon products, such as DHA or TAR, in the output anolyte stream. In addition, this enhancement is observed even at high and commercially relevant current densities of 200 mA cm^{-2}. This can be attributed not only to the shorter residence time in the alkaline anolyte prior to neutralization with H_2SO_4 but also to a change in the reaction mechanism due to the presence of adsorbed Bi species during the electrochemical experiments. Interestingly, at a current density of −90 mA·cm^{-2}, the presence of Bi_2O_3 in the anolyte also induces a slight improvement of the EC, FE, and $HCOO^-$ concentration during the continuous CO_2 electroreduction toward formate. Despite obtaining these promising results in the continuous coelectrovalorization of CO_2 and glycerol, more work specifically oriented to the use of humidified CO_2 streams at the cathode in order to obtain higher $HCOO^-$ concentrations is still required.[64] This continuous CO_2 electroreduction using humidified CO_2 streams should be also coupled with improvements in the GOR to produce higher-value three-carbon products.

ASSOCIATED CONTENT

Supporting Information

The Supporting Information is available free of charge at https://pubs.acs.org/doi/10.1021/acssuschemeng.3c07131.

Experimental details for voltammetric studies, description of the analytical techniques used for the quantification of products, details of the main figures of merit used, oxidation reactions of glycerol to the different products, $ERCO_2$ and comparison with previous papers, voltammetric response of the Pt/C-PE in 0.5 M H_2SO_4 and in 1 M KOH with and without GLY, different glycerol oxidation products, infrared spectra, and calibration plot for the quantification of glycerol in the anolyte output stream, and carbon balance for the anolyte stream in the presence of Bi_2O_3 at different current densities (PDF)

AUTHOR INFORMATION

Corresponding Author

Jose Solla-Gullón − *Instituto de Electroquímica, Universidad de Alicante, E-03080 Alicante, Spain*; Email: jose.solla@ua.es

Authors

Ailen Peña-Rodríguez − *Instituto de Electroquímica, Universidad de Alicante, E-03080 Alicante, Spain*

Kevin Fernández-Caso − *Departamento de Ingenierías Química y Biomolecular, Universidad de Cantabria, 39005 Santander, Spain*

Guillermo Díaz-Sainz − *Departamento de Ingenierías Química y Biomolecular, Universidad de Cantabria, 39005 Santander, Spain*

Manuel Álvarez-Guerra − *Departamento de Ingenierías Química y Biomolecular, Universidad de Cantabria, 39005 Santander, Spain*; orcid.org/0000-0002-3546-584X

Vicente Montiel − *Instituto de Electroquímica, Universidad de Alicante, E-03080 Alicante, Spain*; orcid.org/0000-0002-9570-8110

Complete contact information is available at: https://pubs.acs.org/10.1021/acssuschemeng.3c07131

Notes

The authors declare no competing financial interest.

ACKNOWLEDGMENTS

The authors gratefully acknowledge the financial support through MCIN/AEI/10.13039/501100011033 projects PID2019-108136RB-C31 and PID2019-108136RB-C32. We also want to express our deepest gratitude to Prof. Angel Irabien for his trust, support, and exceptional work as head of the DePRO research group at UC.

REFERENCES

(1) Stephens, I. E. L.; Chan, K.; Bagger, A.; Boettcher, S. W.; Bonin, J.; Boutin, E.; Buckley, A. K.; Buonsanti, R.; Cave, E. R.; Chang, X.; et al. 2022 Roadmap on Low Temperature Electrochemical CO_2 Reduction. *J. Phys.: Energy* **2022**, *4*, 042003.

(2) Wang, Z.; Zhou, Y.; Qiu, P.; Xia, C.; Fang, W.; Jin, J.; Huang, L.; Deng, P.; Su, Y. Q.; Crespo-Otero, R.; Tian, X.; You, B.; Guo, W.; Di Tommaso, D.; Pang, Y.; Ding, S.; Xia, B. Y. Advanced Catalyst Design and Reactor Configuration Upgrade in Electrochemical Carbon Dioxide Conversion. *Adv. Mater.* **2023**, *35*, 2303052.

(3) Liu, L.; Wu, X.; Wang, F.; Zhang, L.; Wang, X.; Song, S.; Zhang, H. Dual-Site Metal Catalysts for Electrocatalytic CO_2 Reduction Reaction. *Chem.—Eur. J.* **2023**, *29* (49), No. e202300583.

(4) Ampelli, C.; Tavella, F.; Giusi, D.; Ronsisvalle, A. M.; Perathoner, S.; Centi, G. Electrode and Cell Design for CO_2 Reduction: A Viewpoint. *Catal. Today* **2023**, *421*, 114217.

(5) Fernández-Caso, K.; Díaz-Sainz, G.; Alvarez-Guerra, M.; Irabien, A. Electroreduction of CO_2: Advances in the Continuous Production of Formic Acid and Formate. *ACS Energy Lett.* **2023**, *8*, 1992−2024.

(6) Yang, P. P.; Gao, M. R. Enrichment of Reactants and Intermediates for Electrocatalytic CO_2 Reduction. *Chem. Soc. Rev.* **2023**, *52* (13), 4343−4380.

(7) Gong, Y.; He, T. Gaining Deep Understanding of Electrochemical CO_2RR with In Situ/Operando Techniques. *Small Methods* **2023**, *7*, 2300702.

(8) Habibzadeh, F.; Mardle, P.; Zhao, N.; Riley, H. D.; Salvatore, D. A.; Berlinguette, C. P.; Holdcroft, S.; Shi, Z. Ion Exchange Membranes in Electrochemical CO_2 Reduction Processes. *Electrochem. Energy Rev.* **2023**, *6*, 26.

(9) Zhang, Z.; Huang, X.; Chen, Z.; Zhu, J.; Endrődi, B.; Janáky, C.; Deng, D. Membrane Electrode Assembly for Electrocatalytic CO_2 Reduction: Principle and Application. *Angew. Chem., Int. Ed.* **2023**, *62* (28), No. e202302789.

(10) Qiu, Z.; Yun, Y.; He, M.; Wang, L. Recent Developments in Ion Conductive Membranes for CO_2 Electrochemical Reduction. *Chem. Eng. J.* **2023**, *456*, 140942.

(11) Duan, Y. X.; Cui, R. C.; Jiang, Q. Recent Progress on the Electroreduction of Carbon Dioxide to C1 Liquid Products. *Curr. Opin. Electrochem.* **2023**, *38*, 101219.

(12) Yan, Z.; Liu, W.; Liu, X.; Shen, Z.; Li, X.; Cao, D. Recent Progress in Electrocatalytic Conversion of CO_2 to Valuable C_2 Products. *Adv. Mater. Interfaces* **2023**, *10* (20), 2300186.

(13) Lai, W.; Qiao, Y.; Wang, Y.; Huang, H. Stability Issues in Electrochemical CO_2 Reduction: Recent Advances in Fundamental Understanding and Design Strategies. *Adv. Mater.* **2023**, *35*, 2306288.

(14) Chen, Q.; Wang, X.; Zhou, Y.; Tan, Y.; Li, H.; Fu, J.; Liu, M. Electrocatalytic CO_2 Reduction to $C2^+$ Products in Flow Cells. *Adv. Mater.* **2024**, *36*, 2303902.
(15) Yan, T.; Chen, X.; Kumari, L.; Lin, J.; Li, M.; Fan, Q.; Chi, H.; Meyer, T. J.; Zhang, S.; Ma, X. Multiscale CO_2 Electrocatalysis to $C2^+$ Products: Reaction Mechanisms, Catalyst Design, and Device Fabrication. *Chem. Rev.* **2023**, *123* (17), 10530−10583.
(16) Álvarez-Gómez, J. M.; Varela, A. S. Review on Long-Term Stability of Electrochemical CO_2 Reduction. *Energy Fuels* **2023**, *37*, 15283.
(17) Yuan, L.; Zeng, S.; Zhang, X.; Ji, X.; Zhang, S. Advances and Challenges of Electrolyzers for Large-Scale CO_2 Electroreduction. *Mater. Rep.: Energy* **2023**, *3* (1), 100177.
(18) He, R.; Xu, N.; Hasan, I. M. U.; Peng, L.; Li, L.; Huang, H.; Qiao, J. Advances in Electrolyzer Design and Development for Electrochemical CO_2 Reduction. *EcoMat* **2023**, *5* (7), No. e12346.
(19) Lin, J.; Zhang, Y.; Xu, P.; Chen, L. CO_2 Electrolysis: Advances and Challenges in Electrocatalyst Engineering and Reactor Design. *Mater. Rep.: Energy* **2023**, *3* (2), 100194.
(20) Wang, H.; Xue, J.; Liu, C.; Chen, Z.; Li, C.; Li, X.; Zheng, T.; Jiang, Q.; Xia, C. CO_2 Electrolysis toward Acetate: A Review. *Curr. Opin. Electrochem.* **2023**, *39*, 101253.
(21) Chen, T. W.; Chen, S. M.; Anushya, G.; Kannan, R.; G Al-Sehemi, A.; Alargarsamy, S.; Gajendran, P.; Ramachandran, R. Development of Different Kinds of Electrocatalyst for the Electrochemical Reduction of Carbon Dioxide Reactions: An Overview. *Molecules* **2023**, *28* (20), 7016.
(22) Adegoke, K. A.; Maxakato, N. W. Electrocatalytic CO_2 Conversion on Metal-Organic Frameworks Derivative Electrocatalysts. *J. CO2 Util.* **2023**, *69*, 102412.
(23) Ding, M.; Chen, Z.; Liu, C.; Wang, Y.; Li, C.; Li, X.; Zheng, T.; Jiang, Q.; Xia, C. Electrochemical CO_2 Reduction: Progress and Opportunity with Alloying Copper. *Mater. Rep.: Energy* **2023**, *3* (1), 100175.
(24) Du, D.; Lan, R.; Humphreys, J.; Tao, S. Progress in Inorganic Cathode Catalysts for Electrochemical Conversion of Carbon Dioxide into Formate or Formic Acid. *J. Appl. Electrochem.* **2017**, *47* (6), 661−678.
(25) Han, N.; Ding, P.; He, L.; Li, Y.; Li, Y. Promises of Main Group Metal-Based Nanostructured Materials for Electrochemical CO2 Reduction to Formate. *Adv. Energy Mater.* **2020**, *10* (11), 1902338.
(26) An, X.; Li, S.; Hao, X.; Xie, Z.; Du, X.; Wang, Z.; Hao, X.; Abudula, A.; Guan, G. Common Strategies for Improving the Performances of Tin and Bismuth-Based Catalysts in the Electrocatalytic Reduction of CO2 to Formic Acid/Formate. *Renewable Sustainable Energy Rev.* **2021**, *143*, 110952.
(27) Al-Tamreh, S. A.; Ibrahim, M. H.; El-Naas, M. H.; Vaes, J.; Pant, D.; Benamor, A.; Amhamed, A. Electroreduction of Carbon Dioxide into Formate: A Comprehensive Review. *ChemElectroChem* **2021**, *8* (17), 3207−3220.
(28) Kuang, Y.; Rabiee, H.; Ge, L.; Rufford, T. E.; Yuan, Z.; Bell, J.; Wang, H. High-Concentration Electrosynthesis of Formic Acid/Formate from CO_2: Reactor and Electrode Design Strategies. *Energy Environ. Mater.* **2023**, *6* (6), No. e12596.
(29) Zou, J.; Liang, G.; Lee, C.-Y.; Wallace, G. G. Progress and perspectives for electrochemical CO2 reduction to formate. *Mater. Today Energy* **2023**, *38*, 101433.
(30) Ewis, D.; Arsalan, M.; Khaled, M.; Pant, D.; Ba-Abbad, M. M.; Amhamed, A.; El-Naas, M. H. Electrochemical reduction of CO2 into formate/formic acid: A review of cell design and operation. *Sep. Purif. Technol.* **2023**, *316*, 123811.
(31) Ma, D.; Jin, T.; Xie, K.; Huang, H. An Overview of Flow Cell Architecture Design and Optimization for Electrochemical CO_2 Reduction. *J. Mater. Chem. A* **2021**, *9* (37), 20897−20918.
(32) Weekes, D. M.; Salvatore, D. A.; Reyes, A.; Huang, A.; Berlinguette, C. P.; Blusson, S. Electrolytic CO_2 Reduction in a Flow Cell. *Acc. Chem. Res.* **2018**, *51* (4), 910−918.
(33) Nicholls, T. P.; Schotten, C.; Willans, C. E. Electrochemistry in Continuous Systems. *Curr. Opin. Green Sustainable Chem.* **2020**, *26*, 100355.
(34) García de Arquer, F. P.; Dinh, C. T.; Ozden, A.; Wicks, J.; McCallum, C.; Kirmani, A. R.; Nam, D. H.; Gabardo, C.; Seifitokaldani, A.; Wang, X.; Li, Y. C.; Li, F.; Edwards, J.; Richter, L. J.; Thorpe, S. J.; Sinton, D.; Sargent, E. H. CO_2 Electrolysis to Multicarbon Products at Activities Greater than 1 A cm^{-2}. *Science* **2020**, *367* (6478), 661−666.
(35) Huang, J. E.; Li, F.; Ozden, A.; Sedighian Rasouli, A.; García de Arquer, F. P.; Liu, S.; Zhang, S.; Luo, M.; Wang, X.; Lum, Y.; Xu, Y.; Bertens, K.; Miao, R. K.; Dinh, C. T.; Sinton, D.; Sargent, E. H. CO_2 Electrolysis to Multicarbon Products in Strong Acid. *Science* **2021**, *372* (6546), 1074−1078.
(36) Li, L.; Ozden, A.; Guo, S.; García de Arquer, F. P.; Wang, C.; Zhang, M.; Zhang, J.; Jiang, H.; Wang, W.; Dong, H.; Sinton, D.; Sargent, E. H.; Zhong, M. Stable, Active CO_2 Reduction to Formate via Redox-Modulated Stabilization of Active Sites. *Nat. Commun.* **2021**, *12* (1), 5223.
(37) Sabatino, S.; Galia, A.; Saracco, G.; Scialdone, O. Development of an Electrochemical Process for the Simultaneous Treatment of Wastewater and the Conversion of Carbon Dioxide to Higher Value Products. *ChemElectroChem* **2017**, *4* (1), 150−159.
(38) Verma, S.; Lu, S.; Kenis, P. J. A. Co-Electrolysis of CO_2 and Glycerol as a Pathway to Carbon Chemicals with Improved Technoeconomics Due to Low Electricity Consumption. *Nat. Energy* **2019**, *4* (6), 466−474.
(39) Houache, M. S. E.; Safari, R.; Nwabara, U. O.; Rafaïdeen, T.; Botton, G. A.; Kenis, P. J. A.; Baranton, S.; Coutanceau, C.; Baranova, E. A. Selective Electrooxidation of Glycerol to Formic Acid over Carbon Supported $Ni_{1-x}M_x$(M = Bi, Pd, and Au) Nanocatalysts and Coelectrolysis of CO_2. *ACS Appl. Energy Mater.* **2020**, *3* (9), 8725−8738.
(40) Hauke, P.; Brückner, S.; Strasser, P. Paired Electrocatalytic Valorization of CO_2 and Hydroxymethylfurfural in a Noble Metal-Free Bipolar Membrane Electrolyzer. *ACS Sustain. Chem. Eng.* **2023**, *11* (37), 13628−13635.
(41) Fernández-Caso, K.; Peña-Rodríguez, A.; Solla-Gullón, J.; Montiel, V.; Díaz-Sainz, G.; Alvarez-Guerra, M.; Irabien, A. Continuous Carbon Dioxide Electroreduction to Formate Coupled with the Single-Pass Glycerol Oxidation to High Value-Added Products. *J. CO2 Util.* **2023**, *70*, 102431.
(42) Li, D.; Yang, J.; Lian, J.; Yan, J.; Frank Liu, S. Recent Advances in Paired Electrolysis Coupling CO_2 Reduction with Alternative Oxidation Reactions. *J. Energy Chem.* **2023**, *77*, 406−419.
(43) Junqueira, J. R. C.; Das, D.; Cathrin Brix, A.; Dieckhöfer, S.; Weidner, J.; Wang, X.; Shi, J.; Schuhmann, W. Simultaneous Anodic and Cathodic Formate Production in a Paired Electrolyzer by CO_2 Reduction and Glycerol Oxidation. *ChemSusChem* **2023**, *16* (11), No. e202202349.
(44) Xi, W.; Yang, P.; Jiang, M.; Wang, X.; Zhou, H.; Duan, J.; Ratova, M.; Wu, D. Electrochemical CO_2 Reduction Coupled with Alternative Oxidation Reactions: Electrocatalysts, Electrolytes, and Electrolyzers. *Appl. Catal., B* **2024**, *341*, 123291.
(45) Tian, J.; Cao, C.; Ma, D.-D.; Han, S.-G.; He, Y.; Wu, X.-T.; Zhu, Q.-L. Killing Two Birds with One Stone: Selective Oxidation of Small Organic Molecule as Anodic Reaction to Boost CO_2 Electrolysis. *Small Struct.* **2022**, *3* (5), 2100134.
(46) Wang, G.; Chen, J.; Li, K.; Huang, J.; Huang, Y.; Liu, Y.; Hu, X.; Zhao, B.; Yi, L.; Jones, T. W.; Wen, Z. Cost-Effective and Durable Electrocatalysts for Co-Electrolysis of CO_2 Conversion and Glycerol Upgrading. *Nano Energy* **2022**, *92*, 106751.
(47) Li, M.; Wang, T.; Zhao, W.; Wang, S.; Zou, Y. A Pair-Electrosynthesis for Formate at Ultra-Low Voltage Via Coupling of CO_2 Reduction and Formaldehyde Oxidation. *Nano-Micro Lett.* **2022**, *14* (1), 211.
(48) Vass, A.; Kormányos, A.; Kószó, Z.; Endrődi, B.; Janáky, C. Anode Catalysts in CO_2 Electrolysis: Challenges and Untapped Opportunities. *ACS Catal.* **2022**, *12* (2), 1037−1051.

https://doi.org/10.1021/acssuschemeng.3c07131
ACS Sustainable Chem. Eng. 2024, 12, 3671−3679

(49) Xu, Z.; Peng, C.; Zheng, G. Coupling Value-Added Anodic Reactions with Electrocatalytic CO_2 Reduction. *Chem.—Eur. J.* **2023**, *29* (11), No. e202203147.
(50) Zhong, W.; Huang, W.; Ruan, S.; Zhang, Q.; Wang, Y.; Xie, S. Electrocatalytic Reduction of CO_2 Coupled with Organic Conversion to Selectively Synthesize High-Value Chemicals. *Chem.—Eur. J.* **2023**, *29* (20), No. e202203228.
(51) Pei, Y.; Pi, Z.; Zhong, H.; Cheng, J.; Jin, F. Glycerol Oxidation-Assisted Electrochemical CO_2 Reduction for the Dual Production of Formate. *J. Mater. Chem. A* **2022**, *10* (3), 1309−1319.
(52) Vehrenberg, J.; Baessler, J.; Decker, A.; Keller, R.; Wessling, M. Paired Electrochemical Synthesis of Formate via Oxidation of Glycerol and Reduction of CO_2 in a Flow Cell Reactor. *Electrochem. Commun.* **2023**, *151*, 107497.
(53) van den Bosch, B.; Rawls, B.; Brands, M. B.; Koopman, C.; Phillips, M. F.; Figueiredo, M. C.; Gruter, G. J. M. Formate Over-Oxidation Limits Industrialization of Glycerol Oxidation Paired with Carbon Dioxide Reduction to Formate. *ChemPlusChem* **2023**, *88* (4), No. e202300112.
(54) Dodekatos, G.; Schünemann, S.; Tüysüz, H. Recent Advances in Thermo-Photo-and Electrocatalytic Glycerol Oxidation. *ACS Catal.* **2018**, *8* (7), 6301−6333.
(55) Braun, M.; Santana, C. S.; Garcia, A. C.; Andronescu, C. From Waste to Value - Glycerol Electrooxidation for Energy Conversion and Chemical Production. *Curr. Opin. Green Sustainable Chem.* **2023**, *41*, 100829.
(56) Tuleushova, N.; Holade, Y.; Cornu, D.; Tingry, S. Glycerol Electro-Reforming in Alkaline Electrolysis Cells for the Simultaneous Production of Value-Added Chemicals and Pure Hydrogen - Mini-Review. *Electrochem. Sci. Adv.* **2023**, *3* (2), No. e2100174.
(57) Wu, J.; Yang, X.; Gong, M. Recent Advances in Glycerol Valorization via Electrooxidation: Catalyst, Mechanism and Device. *Chin. J. Catal.* **2022**, *43* (12), 2966−2986.
(58) Rumayor, M.; Dominguez-Ramos, A.; Irabien, A. Feasibility Analysis of a CO_2 Recycling Plant for the Decarbonization of Formate and Dihydroxyacetone Production. *Green Chem.* **2021**, *23*, 4840−4851.
(59) Coutanceau, C.; Baranton, S.; Kouamé, R. S. B. Selective Electrooxidation of Glycerol into Value-Added Chemicals: A Short Overview. *Front. Chem.* **2019**, *7* (2), 100.
(60) Angelucci, C. A.; Souza-Garcia, J.; Fernández, P. S.; Santiago, P. V. B.; Sandrini, R. M. L. M. Glycerol Electrooxidation on Noble Metal Electrode Surfaces. *Encyclopedia of Interfacial Chemistry: Surface Science and Electrochemistry*; Elsevier, 2020, pp 643−650.
(61) Fan, L.; Liu, B.; Liu, X.; Senthilkumar, N.; Wang, G.; Wen, Z. Recent Progress in Electrocatalytic Glycerol Oxidation. *Energy Technol.* **2021**, *9* (2), 2000804.
(62) Shubair, A.; Houache, M. S. E.; Mousavi M, S. S.; Botton, G. A.; Baranova, E. A. Electrolysis of Glycerol to Value-Added Chemicals in Alkaline Media. *J. Chem. Technol. Biotechnol.* **2022**, *97* (8), 1950−1958.
(63) Simões, M.; Baranton, S.; Coutanceau, C. Enhancement of Catalytic Properties for Glycerol Electrooxidation on Pt and Pd Nanoparticles Induced by Bi Surface Modification. *Appl. Catal., B* **2011**, *110*, 40−49.
(64) Kwon, Y.; Hersbach, T. J. P.; Koper, M. T. M. Electro-Oxidation of Glycerol on Platinum Modified by Adatoms: Activity and Selectivity Effects. *Top. Catal.* **2014**, *57* (14−16), 1272−1276.
(65) Garcia, A. C.; Birdja, Y. Y.; Tremiliosi-Filho, G.; Koper, M. T. M. Glycerol Electro-Oxidation on Bismuth-Modified Platinum Single Crystals. *J. Catal.* **2017**, *346*, 117−124.
(66) De Souza, M. B. C.; Vicente, R. A.; Yukuhiro, V. Y.; V M T Pires, C. T. G.; Cheuquepán, W.; Bott-Neto, J. L.; Solla-Gullón, J.; Fernández, P. S. Bi-Modified Pt Electrodes toward Glycerol Electrooxidation in Alkaline Solution: Effects on Activity and Selectivity. *ACS Catal.* **2019**, *9* (6), 5104−5110.
(67) De Souza, M. B. C.; Yukuhiro, V. Y.; Vicente, R. A.; Vilela Menegaz Teixeira Pires, C. T. G.; Bott-Neto, J. L.; Fernández, P. S. Pb- and Bi-Modified Pt Electrodes toward Glycerol Electrooxidation in Alkaline Media. Activity, Selectivity, and the Importance of the Pt Atoms Arrangement. *ACS Catal.* **2020**, *10* (3), 2131−2137.
(68) Ferreira, D. S.; Gaiotti, A. C.; Araujo, H. R.; Batista, B. C.; Reis, D. D.; Janete Giz, M.; Camara, G. A. Electro-Oxidation of Glycerol over Sb-Modified Pt (1 0 0) Preferentially Oriented Nanoparticles. *J. Catal.* **2023**, *417*, 445−452.
(69) De Souza, M. B. C.; Guima, K. E.; Fernández, P. S.; Martins, C. A. Glycerol Is Converted into Energy and Carbonyl Compounds in a 3D-Printed Microfluidic Fuel Cell: In Situ and in Operando Bi-Modified Pt Anodes. *ACS Appl. Mater. Interfaces* **2022**, *14* (22), 25457−25465.
(70) Díaz-Sainz, G.; Alvarez-Guerra, M.; Solla-Gullón, J.; García-Cruz, L.; Montiel, V.; Irabien, A. CO_2 Electroreduction to Formate: Continuous Single-Pass Operation in a Filter-Press Reactor at High Current Densities Using Bi Gas Diffusion Electrodes. *J. CO2 Util.* **2019**, *34*, 12−19.
(71) Díaz-Sainz, G.; Alvarez-Guerra, M.; Ávila-Bolívar, B.; Solla-Gullón, J.; Montiel, V.; Irabien, A. Improving Trade-Offs in the Figures of Merit of Gas-Phase Single-Pass Continuous CO_2 Electrocatalytic Reduction to Formate. *Chem. Eng. J.* **2021**, *405*, 126965.
(72) Díaz-Sainz, G.; Alvarez-Guerra, M.; Solla-Gullón, J.; García-Cruz, L.; Montiel, V.; Irabien, A. Catalyst Coated Membrane Electrodes for the Gas Phase CO_2 Electroreduction to Formate. *Catal. Today* **2020**, *346*, 58−64.
(73) Díaz-Sainz, G.; Alvarez-Guerra, M.; Irabien, A. Continuous Electroreduction of CO_2 towards Formate in Gas-Phase Operation at High Current Densities with an Anion Exchange Membrane. *J. CO2 Util.* **2022**, *56* (2), 101822.
(74) Del Castillo, A.; Alvarez-Guerra, M.; Solla-Gullón, J.; Sáez, A.; Montiel, V.; Irabien, A. Electrocatalytic Reduction of CO_2 to Formate Using Particulate Sn Electrodes: Effect of Metal Loading and Particle Size. *Appl. Energy* **2015**, *157*, 165−173.
(75) Burdyny, T.; Smith, W. A. CO_2 Reduction on Gas-Diffusion Electrodes and Why Catalytic Performance Must Be Assessed at Commercially Relevant Conditions. *Energy Environ. Sci.* **2019**, *12* (5), 1442−1453.
(76) Solla-Gullón, J.; Rodríguez, P.; Herrero, E.; Aldaz, A.; Feliu, J. M. Surface Characterization of Platinum Electrodes. *Phys. Chem. Chem. Phys.* **2008**, *10* (10), 1359−1373.
(77) Vidal-Iglesias, F. J.; Arán-Ais, R. M.; Solla-Gullón, J.; Herrero, E.; Feliu, J. M. Electrochemical Characterization of Shape-Controlled Pt Nanoparticles in Different Supporting Electrolytes. *ACS Catal.* **2012**, *2* (5), 901−910.
(78) Vivier, V.; Régis, A.; Sagon, G.; Nedelec, J.-Y.; Yu, L. T.; Cachet-Vivier, C. Cyclic voltammetry study of bismuth oxide Bi_2O_3 powder by means of a cavity microelectrode coupled with Raman microspectrometry. *Electrochim. Acta* **2001**, *46* (6), 907−914.
(79) De Souza, M. B. C. Development of p-block adatom-modified platinum electrocatalysts for the electrochemical conversion of glycerol in alkaline medium. Ph.D. Thesis, Universidade Estadual de Campinas, 2022.
(80) Zhou, Y.; Shen, Y.; Piao, J. Sustainable Conversion of Glycerol into Value-Added Chemicals by Selective Electro-Oxidation on Pt-Based Catalysts. *ChemElectroChem* **2018**, *5*, 1636−1643.
(81) Houache, M. S. E.; Hughes, K.; Safari, R.; Botton, G. A.; Baranova, E. A. Modification of Nickel Surfaces by Bismuth: Effect on Electrochemical Activity and Selectivity toward Glycerol. *ACS Appl. Mater. Interfaces* **2020**, *12*, 15095−15107.
(82) Li, J.; Jiang, K.; Bai, S.; Guan, C.; Wei, H.; Chu, H. High Productivity of Tartronate from Electrocatalytic Oxidation of High Concentration Glycerol through Facilitating the Intermediate Conversion. *Appl. Catal., B* **2022**, *317*, 121784.
(83) Zhang, Z.; Xin, L.; Qi, J.; Chadderdon, D. J.; Sun, K.; Warsko, K. M.; Li, W. Selective Electro-Oxidation of Glycerol to Tartronate or Mesoxalate on Au Nanoparticle Catalyst via Electrode Potential Tuning in Anion-Exchange Membrane Electro-Catalytic Flow Reactor. *Appl. Catal., B* **2014**, *147*, 871−878.

https://doi.org/10.1021/acssuschemeng.3c07131
ACS Sustainable Chem. Eng. 2024, 12, 3671−3679